Model Parameter Identification and Validation for Energy Saving Light Bulbs

Alexandru Gabriel Gheorghe, Mihai Eugen Marin
Department of Electrical Engineering
Politehnica University of Bucharest
Bucharest, Romania
alexandru.gheorghe@upb.ro

Abstract: - In the recent years, due to electrical energy reduction need, alternative light sources like Compact Fluorescent Lamps (CFL) and Light Emitting Diode lamps (LED) are replacing the classical incandescent light bulbs. These lamps have the disadvantages of being a significant source of harmonics, although they consume less power. This means that the lightning network should be redesigned taking into account the magnitude of the current harmonic components and of the null current. To this aim, an accurate model easy to build and a fast analysis are very useful. This paper presents three models for different types of energy saving light bulbs, two existing ones and a new implementation, a procedure for model parameters identification and a comparison of the models. Some errors criteria are considered, both qualitative and quantitative. The periodic steady state response is computed using a frequency domain analysis.

Key-Words—current sources models, compact fluorescent lamp, light emitting diode, harmonic balance, frequency domain analysis.

Received: May 27, 2020. Revised: September 16, 2020. Accepted: October 2, 2020. Published: November 1, 2020.

1 Introduction

The use of energy saving light bulbs in recent years, such as Compact Fluorescent (CFL) and Light Emitting Diode (LED) lamps, have reduced greenhouse gas emissions. CFLs and LEDs are known to be important sources of harmonics. Their mass adoption leads to a significant increase of the sources of harmonics in the electricity supply networks, therefore the impact on the power quality needs to be clearly understood. One of the key steps in achieving this objective is the development of energy saving light bulbs harmonic models, suitable for large-scale harmonic studies. Due to harmonics in the power grid, some equipment such as transformers and cables, may be overheated which may lead to premature failure.

This paper is structured in seven sections, followed by acknowledgment and references. In the second section, three models for the energy saving light bulbs are presented. The procedure used for parameter identification of the energy saving light bulbs model developed in this paper is presented in section 3. After that, the models are implemented in Advanced Design System (ADS) software in section 4. The simulation results are presented in section 5 and in section 6 some errors are computed. Finally, the conclusions are outlined in section 7.

2 Energy Saving Light Bulbs Models

Besides the fact that it has to reproduce the measured results, for a circuit model to be useful it must be as simple as possible and easy to implement in a circuit simulation software. Simulation with such a model must be fast, accurate and efficient (from the CPU and memory resources viewpoint).

Several equivalent models for the energy saving light bulbs are available in the literature. In [1] a typical CFL circuit is presented (figure 1) together with an equivalent CFL circuit (figure 2) and a generic CFL circuit is proposed (figure 3).

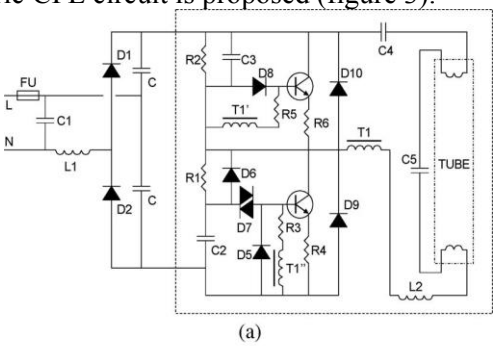

Fig. 1. A typical CFL circuit [1].

These models are simulated in the time domain and the obtained waveforms are very similar to the measurements reported in [1].

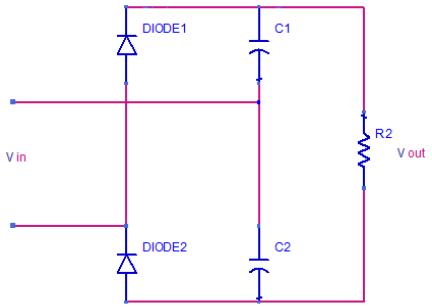

Fig. 2. An equivalent CFL circuit (two diodes rectifier).

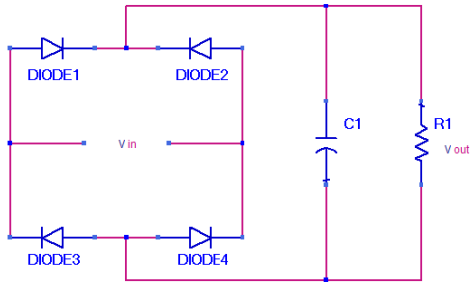

Fig. 3. Equivalent CFL circuit Proposed in [1] (single phase diode bridge rectifier).

In [2] a current source type linear model has been proposed, valid only at a voltage value of 230V RMS, and in its vicinity, since in normal conditions the lamps operate at a constant RMS value of the supply voltage. This model uses current sources controlled by the input voltage. Each current harmonic is described in terms of its amplitude and phase, the control parameters being the magnitude and phase of the fundamental component of the input voltage. This simple model has been implemented and validated through simulations in ADS software using a Frequency Domain Defined 1-Port component (FDD1P). This type of model can be easily used to model other nonlinear home appliance devices [3].

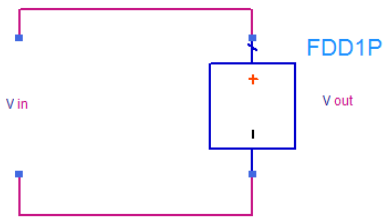

Fig. 4. Linear controlled source model [2].

The FDD1P component, presented in figure 4, is described by the following set of equations where V1 is the input voltage and Ik is the k-th harmonic component of the current.

I1=polar(mag(V1) · 0.06, 0+1· phase(V1))
I3=polar(mag(V1) · 4.02E-02, 183.8+3 · phase(V1))
I5=polar(mag(V1) · 2.21E-2, 35.35+5 · phase(V1))
I7=polar(mag(V1) · 2.40E-2, -102.3+7 · phase(V1))
I9=polar(mag(V1) · 2.07E-2, 90.07+9 · phase(V1))
I11=polar(mag(V1) · 1.02E-2, -55.28+11 · phase(V1))
I13=polar(mag(V1) · 1.26E-2, 192.6+13 · phase(V1))
I15=polar(mag(V1) · 1.58E-2, 20.28+15 · phase(V1))
I17=polar(mag(V1) · 9.32E-3, 227.7+17 · phase(V1))
I19=polar(mag(V1) · 1.02E-2, 108+19 · phase(V1))

The ADS implementation of these equations is presented in figure 5.

```
I[1,1]=polar(mag(_sv(1,1))*0.06/220,-90+135*1+0+1*phase(_sv(1,1)))
I[1,3]=polar(mag(_sv(1,1))*4.02E-02/220, -90+135*3+183.8+3*phase(_sv(1,1)))
I[1,5]=polar(mag(_sv(1,1))*2.21e-2/220, -90+135*5+35.35+5*phase(_sv(1,1)))
I[1,7]=polar(mag(_sv(1,1))*2.40e-2/220, -90+135*7-102.3+7*phase(_sv(1,1)))
I[1,9]=polar(mag(_sv(1,1))*2.07e-2/220, -90+135*9+90.07+9*phase(_sv(1,1)))
I[1,11]=polar(mag(_sv(1,1))*1.02e-2/220, -90+135*11-55.28+11*phase(_sv(1,1)))
I[1,13]=polar(mag(_sv(1,1))*1.26e-2/220, -90+135*13+192.6+13*phase(_sv(1,1)))
I[1,15]=polar(mag(_sv(1,1))*1.58e-2/220, -90+135*15+20.28+15*phase(_sv(1,1)))
I[1,17]=polar(mag(_sv(1,1))*9.32e-3/220, -90+135*17+227.7+17*phase(_sv(1,1)))
I[1,19]=polar(mag(_sv(1,1))*1.02e-2/220, -90+135*19+108+19*phase(_sv(1,1)))
```

Fig. 5. ADS model description [2].

The validity extension of the models developed in [2, 3] is proposed in [4]. This can be done by replicating the current measured not only at the nominal supply network voltage, but for a wide range of RMS values of the supply voltage [190 V, 250 V]. Following the measurements performed on several home appliances, a new current source type model has been suggested. This model will be presented and tested in this paper as it has not been yet validated by implementing it in a circuit simulation software and comparing the results with the measured data.

3 The Procedure for Identifying the Model Parameters

The current harmonic components produced by the energy saving light bulbs have been measured for a RMS value of the supply voltage from 190V to 250V with a 10V step. The variation of the odd RMS current harmonic components up to the 19th harmonic is shown in figure 6 and the variation of the phases with the supply voltage is shown in figure 7.

The dependence with the supply voltage of the most important odd current harmonic components can be computed by linear interpolation, starting from these samples, for both amplitudes and phases.

These equations can be used to simulate the model, for example implementing it in the ADS software.

In order to compare the different models, an absolute error ε_k^a and a relative error ε_k^r can be computed for every considered harmonic

$$\varepsilon_k^a = \left| I_k^s - I_k^m \right| \text{ [A]} \quad (1)$$

$$\varepsilon_k^r = \left| \frac{I_k^s - I_k^m}{I_k^s} \right| \cdot 100 \text{ [\%]} \quad (2)$$

where:

- I_k^s represents the RMS of the k-th current harmonic obtained by simulation, and
- I_k^m represents the RMS of the k-th current harmonic obtained by measurement.

As an overview, the errors can be plotted, or a norm can be computed with the following formulae:

$$\left\| \varepsilon^a \right\| = \sqrt{\sum_{k=1}^{N} \left(\varepsilon_k^a \right)^2} \Big/ N \quad (3)$$

$$\left\| \varepsilon^r \right\| = \sqrt{\sum_{k=1}^{N} \left(\varepsilon_k^r \right)^2} \Big/ N \quad (4)$$

where N is the number of all considered current harmonics and voltage samples.

4 Examples

In this section two types of energy saving light bulbs are modeled, a CFL and a LED.

4.1 The CFL model

Using the procedure described in section 3, a model for a CFL type energy saving light bulb is developed in this section.

The variation of the odd RMS current harmonic components produced by a 10W CFL, up to the 19th harmonic is shown in figure 6 and the variation of the phases with the supply voltage is shown in figure 7. With symbols we represent the measurement points and with a solid line the linear interpolation.

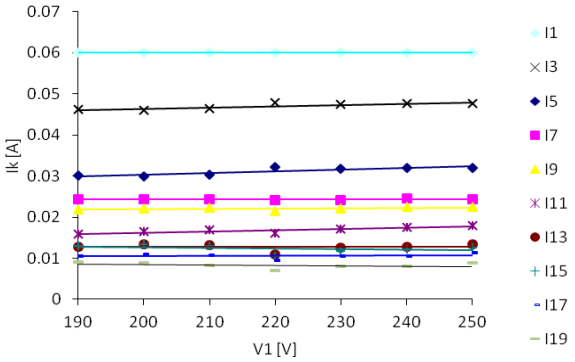

Fig. 6. RMS current harmonics vs. input voltage.

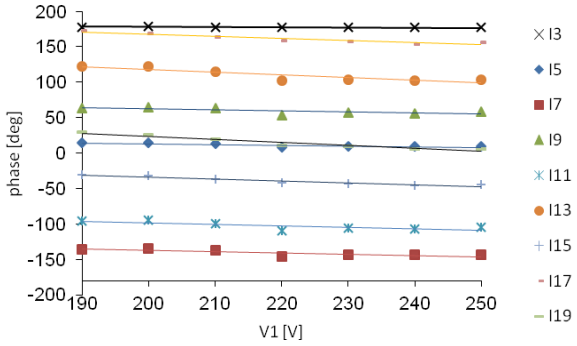

Fig. 7. Phase current harmonics vs. input voltage.

The dependence with the supply voltage of the first 10 odd current harmonic components computed by linear interpolation are presented in the following, both for amplitudes and for phases:

mag(I1) = 6E-18 · mag(V1) + 0.06 [A]
mag(I3) = 3E-05 · mag(V1) + 0.0402 [A]
mag(I5) = 4E-05 · mag(V1) + 0.0221 [A]
mag(I7) = 2E-06 · mag(V1) + 0.024 [A]
mag(I9) = 7E-06 · mag(V1) + 0.0207 [A]
mag(I11) = 3E-05 · mag(V1) + 0.0102 [A]
mag(I13) = 2E-07 · mag(V1) + 0.0126 [A]
mag(I15) = -2E-05 · mag(V1) + 0.0158 [A]
mag(I17) = 6E-06 · mag(V1) + 0.0093 [A]
mag(I19) = -9E-06 · mag(V1) + 0.0102 [A]

phase(I1) = 0.00 · mag(V1) + 0.000 [°]
phase(I3) = -2.86E-02 · mag(V1) + 183.860 [°]
phase(I5) = -1.11E-01 · mag(V1) + 35.357 [°]
phase(I7) = -1.75E-01 · mag(V1) - 102.360 [°]
phase(I9) = -1.393E-01 · mag(V1) + 90.071 [°]
phase(I11) = -2.143E-01 · mag(V1) - 55.286 [°]
phase(I13) = -3.75E-01 · mag(V1) + 192.640 [°]
phase(I15) = -2.714E-01 · mag(V1) + 20.286 [°]
phase(I17) = -3.00E-01 · mag(V1) + 227.710 [°]
phase(I19) = -4.214E-01 · mag(V1) + 108.000 [°]

These equations have been implemented in the ADS software as is shown in figure 8:

```
I[1,1]=polar(6e-18*mag(_sv(1,1))+0.06,-90+135*1+0+1*phase(_sv(1,1)))
I[1,3]=polar(3.09e-5*mag(_sv(1,1))+4.02E-02, -90+135*3+183.8-0.028*mag(_sv(1,1))+3*phase(_sv(1,1)))
I[1,5]=polar(4.11e-5*mag(_sv(1,1))+2.21e-2, -90+135*5+35.35-0.110*mag(_sv(1,1))+5*phase(_sv(1,1)))
I[1,7]=polar(1.50e-6*mag(_sv(1,1))+2.40e-2, -90+135*7-102.3-0.175*mag(_sv(1,1))+7*phase(_sv(1,1)))
I[1,9]=polar(6.64e-6*mag(_sv(1,1))+2.07e-2, -90+135*9+90.07-0.139*mag(_sv(1,1))+9*phase(_sv(1,1)))
I[1,11]=polar(3.04e-5*mag(_sv(1,1))+1.02e-2, -90+135*11-55.28-0.214*mag(_sv(1,1))+11*phase(_sv(1,1)))
I[1,13]=polar(2.14e-7*mag(_sv(1,1))+1.26e-2, -90+135*13+192.6-0.375*mag(_sv(1,1))+13*phase(_sv(1,1)))
I[1,15]=polar(-1.59e-5*mag(_sv(1,1))+1.58e-2, -90+135*15+20.28-0.271*mag(_sv(1,1))+15*phase(_sv(1,1)))
I[1,17]=polar(5.79e-6*mag(_sv(1,1))+9.32e-3, -90+135*17+227.7-0.3*mag(_sv(1,1))+17*phase(_sv(1,1)))
I[1,19]=polar(-8.79e-6*mag(_sv(1,1))+1.02e-2, -90+135*19+108-0.421*mag(_sv(1,1))+19*phase(_sv(1,1)))
```

Fig. 8. Proposed model implementation in ADS

4.2 The LED model

The same procedure is used also for a 5W LED type energy saving light bulb. As it can be observed in figure 9 and figure 10, the harmonic response is

visible different from a CFL but the dependence with the input voltage is still linear.

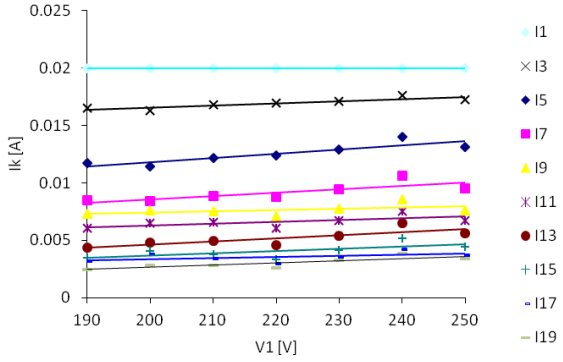

Fig. 9. RMS current harmonics vs. input voltage.

The diference between the measured samples and the linear interpolation, more visible in figure 10, for some harmonic components is due to measurement errors and THD of the input voltage.

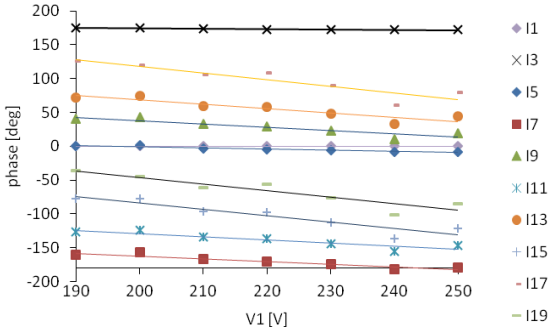

Fig. 10. Phase current harmonics vs. input voltage.

The dependence with the supply voltage of the most important 10 odd current harmonic components has been computed by linear interpolation, both for amplitudes and for phases:

mag(I1) = -1.450E-18 · mag(V1) + 0.02 [A]
mag(I3) = 1.793E-05 · mag(V1) + 1.299E-2 [A]
mag(I5) = 3.629E-05 · mag(V1) + 4.557E-3 [A]
mag(I7) = 2.943E-05 · mag(V1) + 2.680E-3 [A]
mag(I9) = 1.086E-05 · mag(V1) + 5.246E-3 [A]
mag(I11) = 1.564E-05 · mag(V1) + 3.153E-3 [A]
mag(I13) = 2.721E-05 · mag(V1) - 8.186E-4 [A]
mag(I15) = 1.964E-05 · mag(V1) - 2.786E-4 [A]
mag(I17) = 1.864E-05 · mag(V1) - 1.090E-3 [A]
mag(I19) = 9.143E-06 · mag(V1) + 1.529E-3 [A]

phase(I1) = 0.00 · mag(V1) + 0.00 [°]
phase(I3) = -5.710E-02 · mag(V1) + 186.00 [°]
phase(I5) = -1.679E-01 · mag(V1) + 32.643 [°]
phase(I7) = -3.964E-01 · mag(V1) - 82.929 [°]
phase(I9) = -4.893E-01 · mag(V1) + 135.93 [°]
phase(I11) = -4.786E-01 · mag(V1) - 33.143 [°]
phase(I13) = -6.429E-01 · mag(V1) + 197.14 [°]
phase(I15) = -9.464E-01 · mag(V1) + 105.5 [°]
phase(I17) = -9.857E-01 · mag(V1) + 315.29 [°]
phase(I19) = -9.786E-01 · mag(V1) + 149.57 [°]

5 Results

The steady state solution is of interest usually in circuit design. Several methods were developed, either in the time domain or in the frequency domain. The most used method in the time domain is the transient analysis in which the circuit equations are integrated until the transient components decay. Another time domain method is shooting with Newton-Raphson which directly computes the steady state solution generally in 3 up to 5 iterations. Another method that directly computes the steady state solution but in the frequency domain, is the harmonic balance. In the harmonic balance method [5], the nonlinear circuit is split into a linear sub-circuit and a nonlinear sub-circuit. The linear sub-circuit is solved in the frequency domain and the nonlinear one is solved in the time domain. The two sub-circuits are related by the direct and the inverse discrete Fourier transforms. Another frequency domain analysis that directly computes the steady state solution is presented in [6]. For very simple circuits, an analytical approach can be used to find the periodic steady state [7].

5.1 The CFL model

In this paragraph, three CFL models were implemented in the ADS software and their validity has been verified in comparison with the results obtained by amplitude and phase measurements.

By implementing in ADS the model from paper [1], a two diode rectifier, the following graphs are obtained for the odd RMS current harmonic components up to the 19th harmonic (figure 11), and phase for the same harmonic components (figure 12):

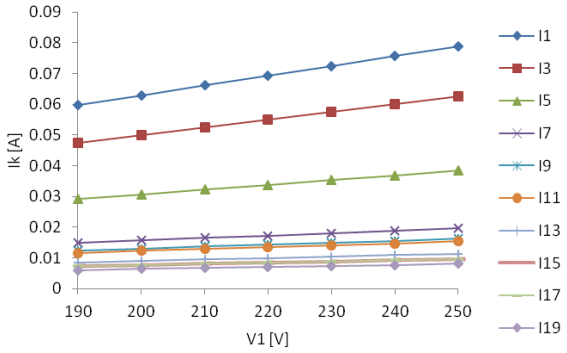

Fig. 11. RMS current harmonics vs. input voltage for the first model.

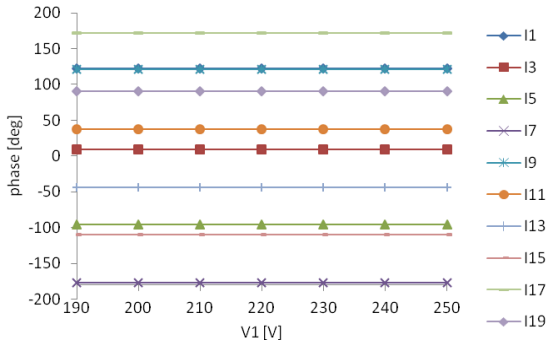

Fig. 12. Phase current harmonics vs. input voltage for the first model.

Using the model from [2] for a CFL, a current source type linear model, the following graphs were obtained for RMS, figure 13, and phase, figure 14:

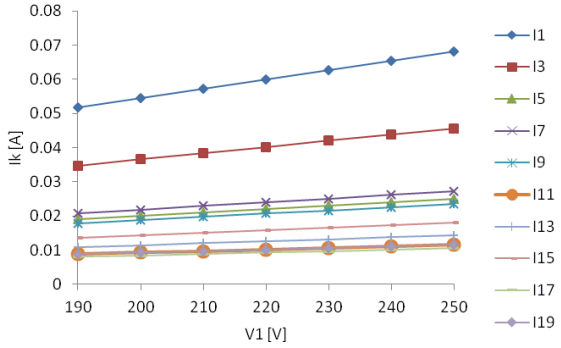

Fig. 13. RMS current harmonics vs. input voltage for the second model.

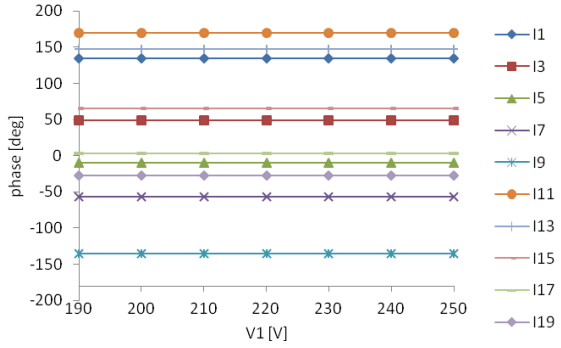

Fig. 14. Phase current harmonics vs. input voltage for the second model.

With the model suggested in [4] and developed in [11], the following graphs were obtained for the RMS value, figure 15, and phase, figure 16:

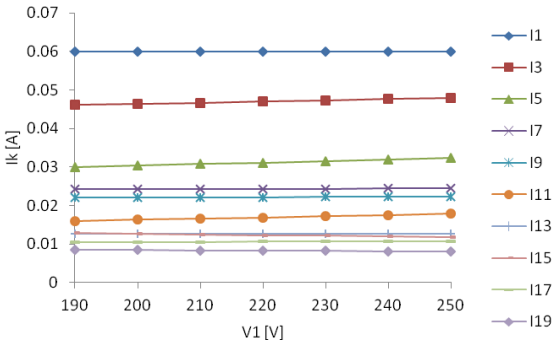

Fig. 15. RMS current harmonics vs. input voltage for the third model.

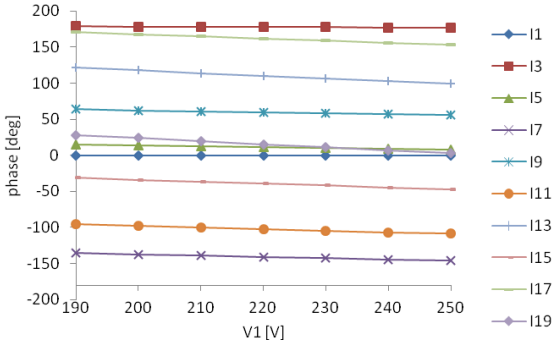

Fig. 16. Phase current harmonics vs. input voltage for the third model.

For a qualitative comparison, below are the measured and the simulated waveforms over the measured RMS input voltage interval.

In figure 17 it can be observed the waveform of the voltage and current, measured for a 10W CFL at a value of 220V RMS of the input voltage.

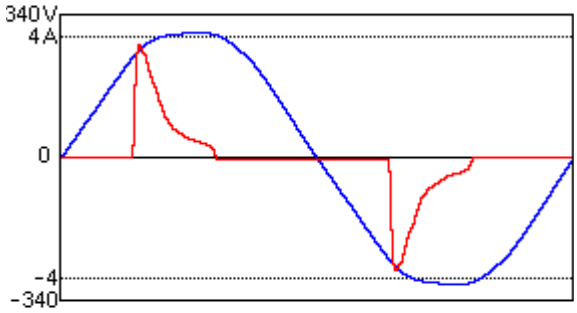

Fig. 17. CFL voltage and current waveform - measured at 220V.

Figure 18 a) shows the simulated waveform of the voltage (in blue) and current (in red) of the first model for a 10W CFL, with a two diodes rectifier. Figure 18 b) shows the simulated current spectrum.

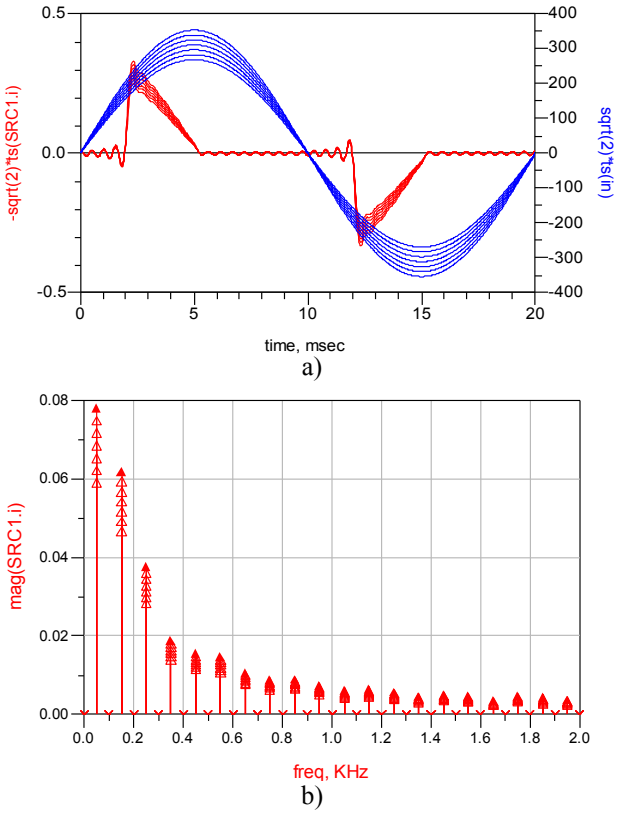

Fig. 18. First model - simulated. a) the voltage and current waveform. b) the current spectrum.

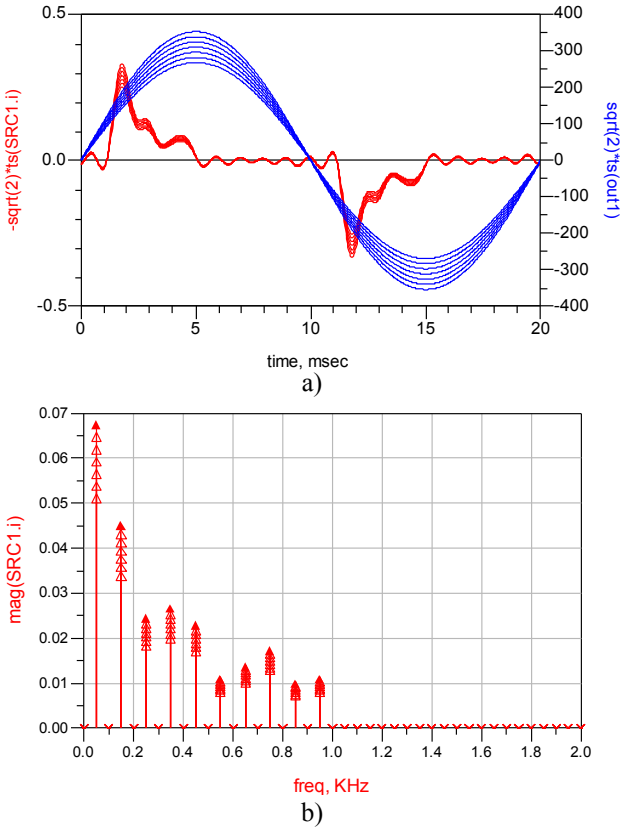

Fig. 19. Second model - simulated. a) the voltage and current waveform. b) the current spectrum.

In figure 19 a) we present the simulated voltage (in blue) and current (in red) waveform of the second model for a 10W CFL, the voltage controlled current source proposed in the paper [2]. Figure 19 b) shows the simulated current spectrum.

Figure 20 a) presents the simulated voltage (in blue) and current (in red) waveform for the voltage controlled current source developed in this paper which also models the same 10W CFL. Figure 20 b) shows the simulated current spectrum.

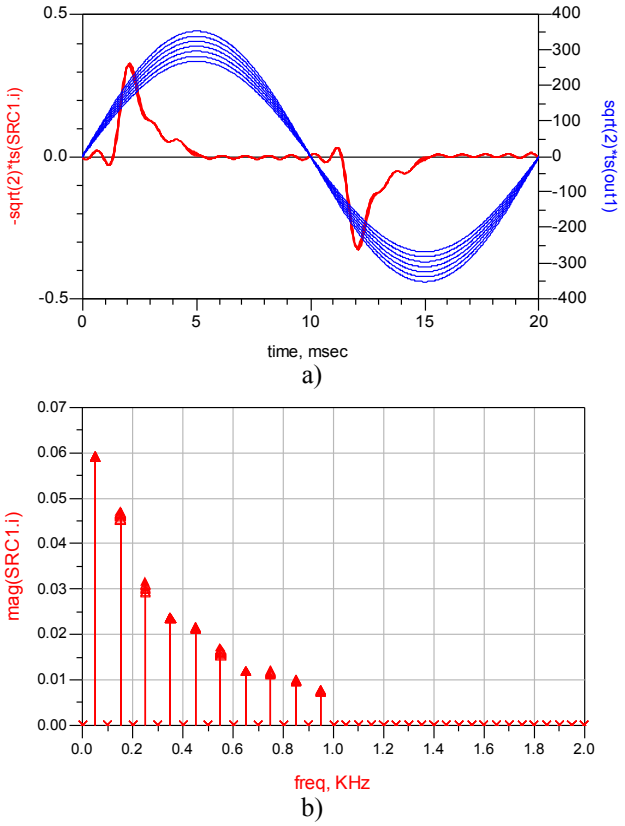

Fig. 20. Third model - simulated. a) the voltage and current waveform. b) the current spectrum.

5.2 The LED model

The same three types of models used to simulate the CFL, are used to simulate a LED energy saving light bulb. The models are implemented also in the ADS software and the obtained results are more or less similar with the ones obtained for the CFL models. The amplitude and phase measurements are used to validate the results obtained by simulation.

The two diode rectifier model from paper [1] leads to the following graphs for the first 10 odd RMS current harmonic components, figure 21, and phase for the same harmonic components figure 22.

Using the second model, the current source type linear model proposed in [2], the following graphs were obtained for RMS, figure 23, and phase, figure 24, of the first 10 odd harmonics.

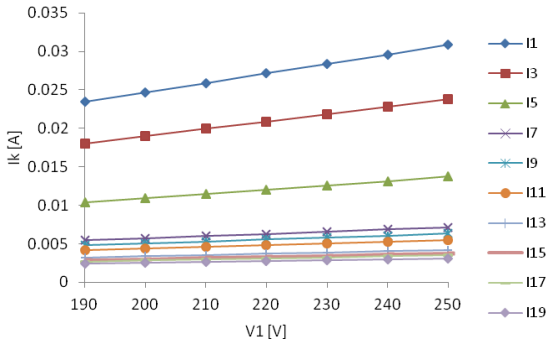

Fig. 21. RMS current harmonics vs. input voltage for the first model.

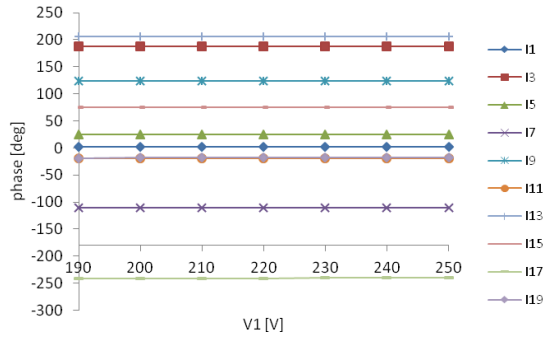

Fig. 22. Phase current harmonics vs. input voltage for the first model.

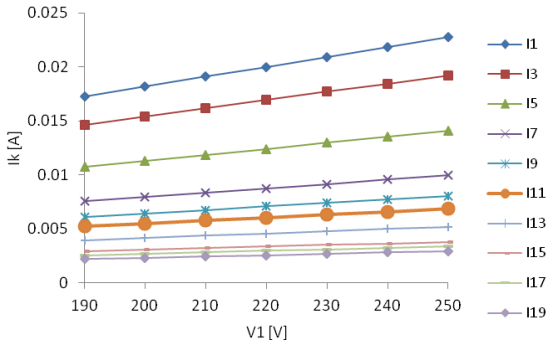

Fig. 23. RMS current harmonics vs. input voltage for the second model.

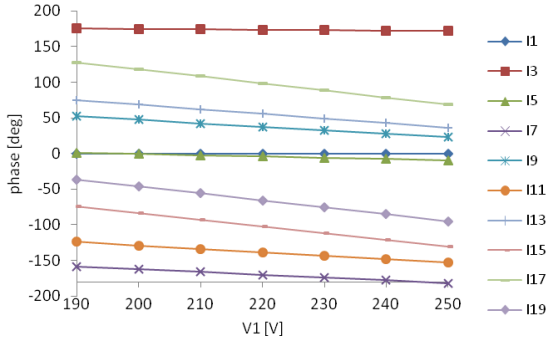

Fig. 24. Phase current harmonics vs. input voltage for the second model.

Finally, but not least, with the model developed in this paper the following graphs are obtained for the RMS value, figure 25 and phase, figure 26, for the same harmonic components.

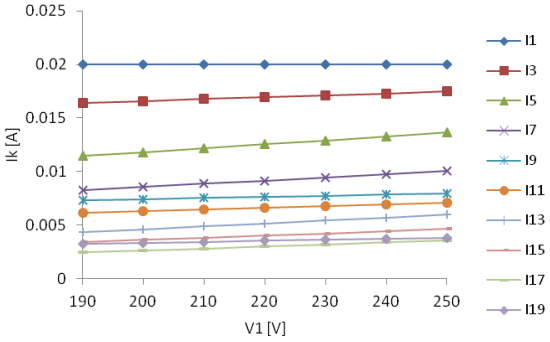

Fig. 25. RMS current harmonics vs. input voltage for the third model.

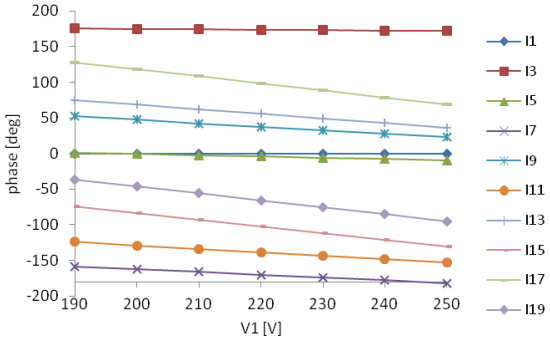

Fig. 26. Phase current harmonics vs. input voltage for the third model.

Below are the measured and the simulated waveforms over the measured RMS input voltage interval.

In figure 27 we observe the waveform of the voltage and current, measured for a 5W LED at a value of the input voltage of 220V RMS.

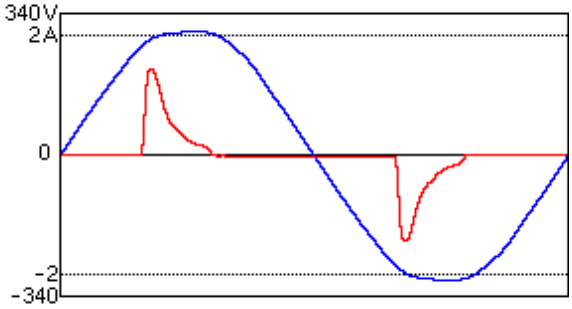

Fig. 27. LED voltage and current waveform - measured at 220V.

Figure 28 a) shows the simulated waveform of the voltage (in blue) and current (in red) of the first model for a 5W LED with a two diodes rectifier. Figure 28 b) shows the simulated current spectrum.

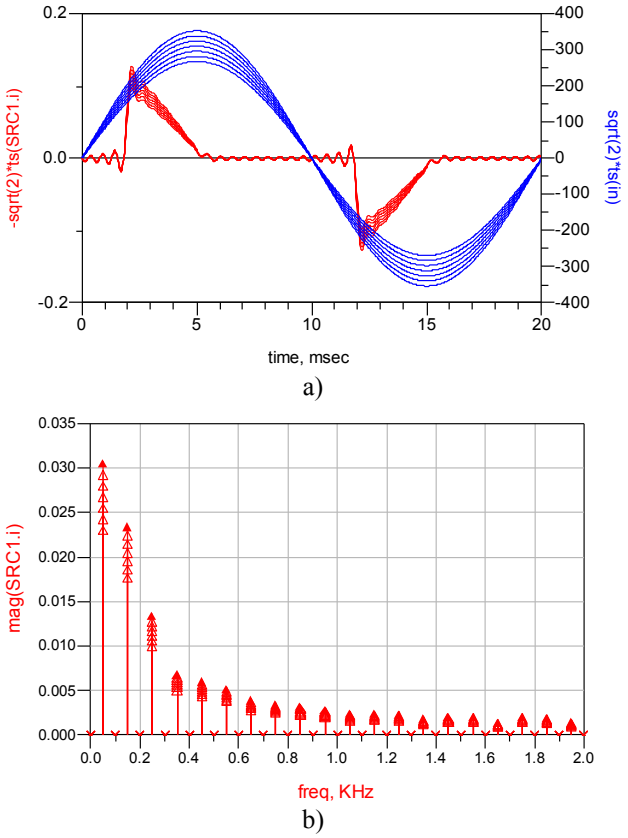

Fig. 28. First model - simulated. a) the voltage and current waveform. b) the current spectrum.

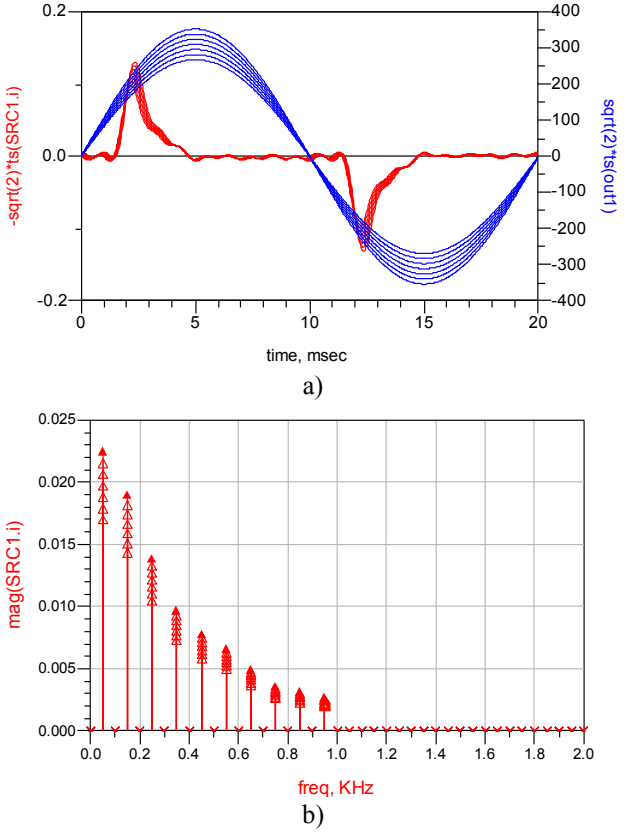

Fig. 29. Second model - simulated. a) the voltage and current waveform. b) the current spectrum.

In figure 29 a) we present the simulated voltage (in blue) and current (in red) waveform of the second model for a 5W LED, the voltage controlled current source proposed in the paper [2]. Figure 29 b) shows the simulated current spectrum.

Figure 30 a) presents the simulated voltage (in blue) and current (in red) waveform for the voltage controlled current source developed in this paper which also models the same 5W LED. Figure 30 b) shows the simulated current spectrum.

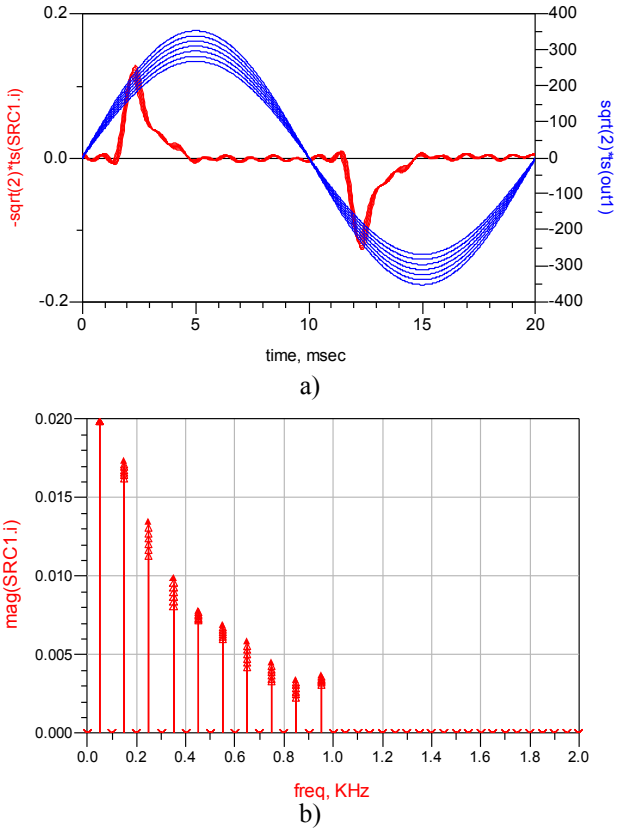

Fig. 30. Third model - simulated. a) the voltage and current waveform. b) the current spectrum.

6 Error computation

Because a large amount of data is hard to follow, the best solution is to display it as a comparative diagram. For example, using the formula (1) for every measured value, would result in 70 points (10 harmonics x 7 voltage samples) only for the RMS of one model. The same is available for formula (2).

6.1 Error computation for the CFL models

The absolute errors computed by (1) for the RMS values of the CFL are presented in figure 31, for all the considered models. In red are presented the errors for the first model, the two diodes rectifier, in blue are the errors for the second model, the current source type linear model, and in green are presented

the errors computed for the third model, developed in this paper.

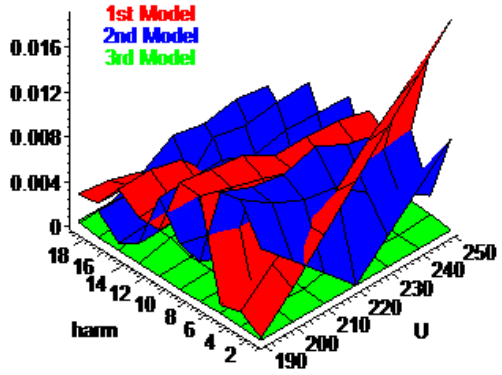

Fig. 31. The absolute errors [A] for the considered models of a CFL

The relative error computed by (2) for the RMS values of the CFL are presented in figure 32.

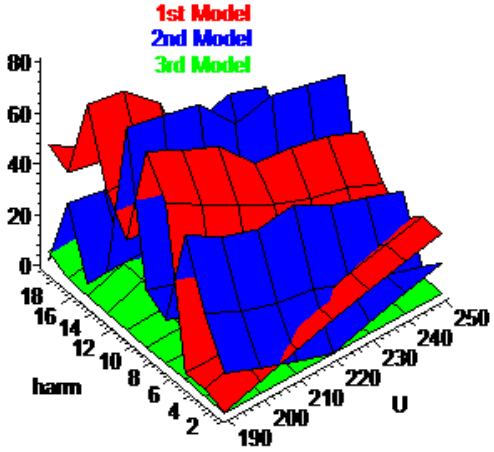

Fig. 32. The relative errors [%] for the considered models of a CFL.

6.2 Error computation for the LED models

The absolute errors computed by (1) for the RMS values for all the considered models of the LED energy saving light bulb are presented in figure 31.

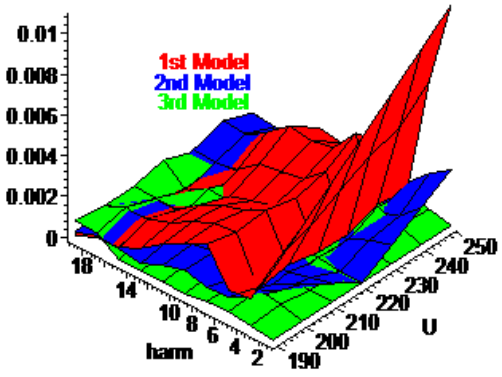

Fig. 33. The absolute errors [A] for the considered models of a LED.

The relative errors computed by (2) for the RMS values of the LED are presented in figure 34.

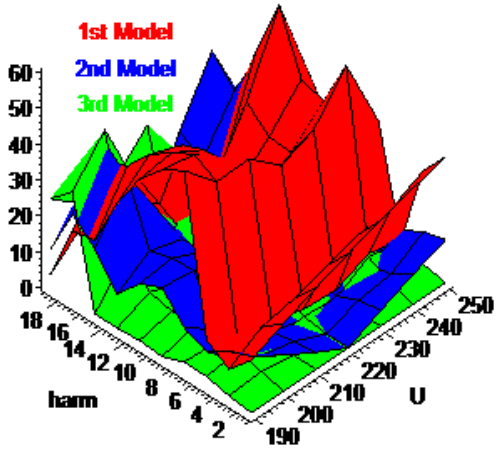

Fig. 34. The relative errors [%] for the considered models of a LED.

From the qualitative point of view, from all the above figures it can be clearly observed that the third model (the green surface) introduces the smallest errors for both types of energy saving light bulbs modeled in this paper.

As an overview, the errors norms computed for the RMS with the (3) and (4) formulae are summarized in Table 1 and Table 2.

Table 1. The RMS absolute errors norms

	1st model	2nd model	3rd model
CFL	7.387E-4	5.974E-4	6.041E-05
LED	3.689E-4	1.097E-4	5.018E-05

Table 2. The RMS relative errors norms

	1st model	2nd model	3rd model
CFL	4.074	3.494	0.497
LED	3.609	1.762	1.252

From the tables above, we observe that the results obtained with the models developed in this paper (the 3rd model) are more accurate than the previously designed ones. It is expected that similar results can be obtained and for the phases of the considered harmonics.

7 Conclusions

Two energy saving light bulbs, a Compact Florescent Lamp (CFL) and a Light Emitting Diode (LED) lamp, have been modeled in this paper by two existing approaches and a new frequency domain model. The new model parameters were obtained by amplitude and phase measurements for all harmonic components of interest (the first 10 odd current harmonics) for an input voltage in the range of [190V, 250V]. The models developed in this work are characterized by an affine dependence between the amplitude of the current harmonic and

the voltage amplitude of the fundamental frequency. This model has been validated by simulations in the voltage range of [190V, 250V], the results obtained being in accordance with the measured ones and more accurate than the previously designed models. The accuracy of the models has been checked by comparative graphical representations and by absolute and relative error computation relative to the measurements. The errors between the measured samples and the linear interpolation used by the models is also due to measurement errors, and the THD (Total Harmonic Distorsion) of the input voltage that introduces suplementary distorsion of the current.

To further improve the accuracy of the model, the number of harmonics considered can be increased. It can be observed that only for the models designed in this paper the current waveform is not influenced by the input voltage variation (figure 20 and figure 30). If the parameters for the analyzed models are computed starting from an extended set of measurements, the validity range of the model can be extended for more than [190V, 250V] of the input voltage. This type of model could be more efficient than some other types of model, like the behavior ones [8].

It was observed that the reduction of the simulation time is greater in case of weakly nonlinear devices in comparison to the classical methods. This makes Frequency Domain (FD) models also suitable to simulate electrical drives [9] in steady state. The current waveform obtained with this approach is similar with those obtained for a variety of energy saving light bulbs models and methods [10, 11].

8 Acknowledgment

The work of Mihai-Eugen Marin has been funded by the Operational Programme Human Capital of the Ministry of European Funds through the Financial Agreement 51675/09.07.2019, SMIS code 125125.

The authors would like to thank Professor Florin Constantinescu for the helpful discussions.

References:

[1] J. Yong, L. Chen, A. Nassif, W. Xu, *A Frequency-Domain Harmonic Model for Compact Fluorescent Lamps*, IEEE Transactions on Power Delivery, vol. 25, No. 2, April 2010, pp 1182-1189.

[2] F. Constantinescu, A. G. Gheorghe, M. E. Marin, O. Taus, *Harmonic balance analysis of home appliances power networks,* 2017 14th International Conference on Engineering of Modern Electric Systems (EMES), June 1-2 2017, Oradea, Romania.

[3] A. G. Gheorghe, F. Constantinescu, M. E. Marin, V. Ştefănescu, G. Vătăşelu, *Frequency Domain Models for Nonlinear Home Appliance Devices*, 2018 International Symposium on Fundamentals of Electrical Engineering (ISFEE), Bucharest, Romania, November 1-2, 2018.

[4] F. Constantinescu, A. G. Gheorghe, M. E. Marin, G. Vătăşelu, V. Ştefănescu, D. Bodescu *New Models for Frequency Domain Simulation of Home Appliances Networks*, 2019 11th International Symposium on Advanced Topics in Electrical Engineering (ATEE), 28-30 March 2019.

[5] Pauli Heikkila, Martti Valtonen, Timo Veijola, *Harmonic balance of nonlinear circuits with multitone excitation*, Proceedings of ECCTD-91.

[6] F. I. Hantila, F. Constantinescu, Al. G. Gheorghe, M. Nitescu, M. Maricaru, *A New Algorithm For Frequency Domain Analysis Of Nonlinear Circuits*, Revue Roumaine des Sciences Techniques-Serie Electrotechnique et Energetique, ISSN: 0035-4066, Vol. 54, Nr. 1, 2009, pp. 57-66, WOS:000264503000006.

[7] K. L. Lian and P. W. Lehn, *Harmonic analysis of single-phase full bridge rectifiers based on fast time domain method*, in ISIE, Montreal, QC, Canada, Jul. 2006, pp. 2608–2613.

[8] F Constantinescu, M Nitescu, AG Gheorghe, A Florea, O Llopis, *Behavioral circuit models of power BAW resonators and filters*, Analog Integrated Circuits and Signal Processing 73 (1), 57-64

[9] Gheorghe, CM., Melcescu, LM, Tudorache, T., Mihai, E. *Numerical modeling approaches for the analysis of squirrel cage induction motor*. Rev. Roum. Sci. Techn. – Électrotechn. et Énerg., vol. 61, nr. 1/2016, p. 18–21, ISSN: 0035-4066.

[10] Z. Wei, N. R. Watson, and L. P. Frater, *Modelling of compact fluorescent lamps*, presented at the ICHQP, Wollongong, Australia, Sep. 2008.

[11] AG Gheorghe, ME Marin, D Bodescu, *Parameter Identification and Model Validation for a Compact Fluorescent Lamp*, 24th International Conference on Circuits, Systems, Communications and Computers (CSCC 2020), Platanias, Chania Crete Island, Greece, July 19-22, 2020.